

## Anisotropy in Elastic Properties of Porous 316L Stainless Steel Due to the Shape and Regular Cell Distribution

M. Mirzaei and M.H. Paydar\*

Department of Materials Science and Engineering, Shiraz University, Shiraz, Iran

### ARTICLE INFO

#### Article history:

Received 8 December 2018  
Revised 23 February 2019  
Accepted 24 February 2019

#### Keywords:

Cell shape  
Regular cell distribution  
Anisotropy  
316L stainless steel foam.

### ABSTRACT

In this study, two-dimensional finite element modeling was used to study the simultaneous effect of the cell shape and regular cell distribution on the anisotropy of the elastic properties of 316L stainless steel foam. In this way, the uniaxial compressive stress-strain curve was predicted using a geometric model and fully solid 316L stainless steel. The results showed that the elastic tangent and the yield strength increase significantly if the direction of the loading is parallel to the major cell dimension. Besides, the regular cell distribution affects the above properties, and the sharp drop in the mechanical properties is observed when the maximum shear stress plane is parallel with the plane including higher cell density. In addition, the finite element modeling showed that the elastic properties of porous 316L stainless steel are anisotropic and the optimum conditions depend entirely on the shape of the cells and the loading direction in the regular cell distribution foam.

© Shiraz University, shiraz, Iran, 2019

### 1. Introduction

Metallic foams have been widely used in a number of potential application fields including damping, heat exchange, sound insulation, and energy absorption [1,2]. However, metallic foams are often anisotropic, i.e. their properties depend on the direction in which they are measured. The heterogeneity and anisotropy measured in foams are generally attributable to the processing methods used in their fabrication. Anisotropy can arise in two quite different ways: structural anisotropy and material anisotropy. The more obvious anisotropic way for metal foams is structural anisotropy: direction-dependent foam properties attributable to the shape of the cells. The cell shape anisotropy can lead to anisotropy in the mechanical properties either for closed-cell or open-cell foams [3,4].

The cell shape anisotropy effect on the compressive properties of metal foams has been investigated by many researchers. Benouali et al reported that Al foams made by the liquid state exhibit a significant anisotropy in their mechanical behavior. In contrast, the foams made by powder metallurgy show an almost isotropic compressive behavior [3]. Mu et al showed that Al–Si foams exhibit higher plastic collapse stress and better energy absorption property in the longitudinal direction (longer cell size) than those in the transverse direction [4–6]. Manonukul et al showed that the degree of geometry anisotropy is not strong enough to result in the mechanical property anisotropy of Ti foam fabricated by replica impregnation method [7].

Recently, in a study carried out by the present authors, it was shown that when the cell distribution is

\* Corresponding author  
E-mail addresses: [paaydar@shirazu.ac.ir](mailto:paaydar@shirazu.ac.ir) (M. H. Paydar)

regular, another type of anisotropy would be created in the compressive properties of the foams, which is similar to what was reported for single crystal materials. In fact, when the cell distribution is regular, the number of cells in each section is different and the mechanical properties would be a function of the loading direction [8,9].

The aim of this work is to investigate the effects of two types of structural anisotropy created by the cell shape and regular cell distribution on the compressive behavior of 316L stainless steel foams using two-dimensional finite element modeling (FEM). For this purpose, the shape of the cells has changed from spherical to elliptic, and by changing the loading direction, the simultaneous effect of the two above-mentioned types of anisotropy are studied.

## 2. Theory of Anisotropy

Figure 1 shows the geometric profile of an elliptical cell. By using orthotropic unit-cell model, Huber and Gibson derived the shape anisotropy ratio  $R$ , as:

$$R = \frac{a}{b} \quad (1)$$

Where  $a$  and  $b$  are the average values of the principal cell dimensions in the  $x$  and  $y$  directions, respectively [10]. According to this, the anisotropic elastic tangent,  $E_x/E_y$ , and yield stress ratio,  $\sigma_x/\sigma_y$ , are defined as:

$$\frac{E_x}{E_y} = \frac{2R^2}{1 + (1/R)^3} + (1 - \varphi) \frac{2R}{1 + (1/R)} \quad (2)$$

$$\frac{\sigma_x}{\sigma_y} = \frac{2R}{1 + (1/R)} \quad (3)$$

Where  $E_x$  and  $E_y$  are the elastic tangent moduli and  $\sigma_x$  and  $\sigma_y$  are the uniaxial yield stresses in the  $x$  and the  $y$  directions, respectively. In this equation,  $\varphi$  is the fraction of solid in the cell edges and bounded by  $\rho^*/\rho_s \leq \varphi \leq 1$ , where  $\rho^*$  and  $\rho_s$  are the densities of the foam and the bulk materials, respectively. One limiting case is when  $\varphi = 1$ , which corresponds to an open-cell foam. For closed-cell foams,  $\varphi$  is less than 1 and smaller values of  $\varphi$  correspond to the foams with thinner cell edges. Usually,  $\varphi$  values between 0.65 and 0.85 are commonly observed [11,12]. Eqs. (2) and (3) predict that the elastic tangent ratio and the yield strength ratio are independent of the relative density and increase by increasing  $R$ .

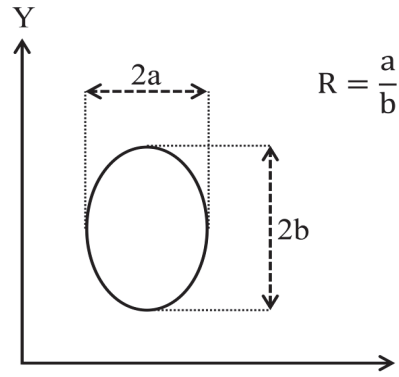


Fig. 1. Specifications and dimensions of the cell geometry

## 3. FEM Procedure

A  $16 \times 18 \text{ cm}^2$  sample with regular cell distribution for FEM simulation was considered. To evaluate the elastic properties of porous 316L stainless steel, the following geometric conditions were applied to the model:

- The number of the cells was considered constant in all cases.
- Changes in the shape of the cells from circle to ellipse were applied in such a way that the area did not change. This condition caused the relative density to be constant in all cases.
- According to the two above-mentioned conditions, the porosity in the samples was considered to be about 60% and constant. Consequently, the relative density was about  $3.2 \text{ g cm}^{-3}$ .
- For boundary condition, uniform displacements were imposed on the faces perpendicular to the loading direction without friction. Other faces parallel to the loading direction were traction free.

By changing  $R$  from 1 (circular cells) to 2.1, the effect of the cell shape anisotropy was investigated. Moreover, by changing the compression loading direction at an angle of  $45^\circ$  with the  $Y$ -axis, the cell distribution anisotropy phenomenon was studied in both the circular and elliptical shapes of the cells. This mode is shown schematically in Fig. 2 In addition, the stress-strain curve data of 316L stainless steel was extracted from the reference [13] and used by Abaqus version

2016 software. A linear elastic behavior was assigned using a Young's Modulus of  $E=200\text{GPa}$  and Poisson ratio of  $\nu = 0.3$ . For the perfect plastic part, the yield stress was 170 MPa and 0.0 plastic strain. Using the software data, the force-displacement curve was converted to the true stress-strain curve and, based on the ISO 13314 standard [14], the yield strength and elastic tangent were calculated.

In this paper, the simplified self-similar yield surface model developed by Deshpande and Fleck, which is available as the crushable foam model in the ABAQUS finite element software, has been employed to describe the deformation behaviour of 316L foam.

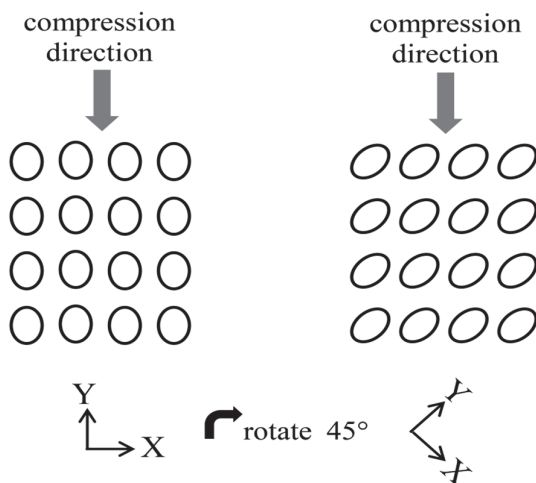


Fig. 2. Schematic of compression loading in two directions; Y-axis and with a  $45^\circ$  angle to the Y-axis

#### 4. Results and Discussion

Figure 3 indicates the contour of the stress for  $R = 1.91$  after 0.5 mm displacement in two loading directions x and y. Comparing Figs. 3a and 3b demonstrates that von Mises stress is higher in the second mode. Regarding these results, it can be concluded that the mechanical properties will improve if the loading is parallel to the major dimension of the cell. This is due to an increase in the stress concentration in the sharp edges of the cells during compression loading.

Here also, it can be shown, similar to the analysis of an elliptical crack, that for a foam containing elliptical cells, the applied stress  $\sigma_a$  is magnified at the

ends of the major axis of the ellipse, so that the following equation is derived:

$$\frac{\sigma_{max}}{\sigma_a} = 1 + \frac{2a}{b} \quad (4)$$

Where  $\sigma_{max}$  and  $\sigma_a$  are the maximum stress at the end of the X-axis and the applied stress perpendicular to the X-axis, respectively. Since the radius of the curvature  $\rho$  at the end of the ellipse is given by

$$\rho = \frac{b^2}{a} \quad (5)$$

Eqs. 4 and 5 may be combined, and then we have:

$$\sigma_{max} = \sigma_a(1 + 2\sqrt{a/\rho}) = \sigma_a k_t \quad (6)$$

The term  $\sigma_{max}/\sigma_a$  is defined as the stress-concentration factor;  $k_t$ , and it describes the effect of the cell geometry. Accordingly, when the applied stress is perpendicular to the major length of the cell, the curvature radius reduces, and therefore the stress concentration increases [15]. Accordingly, in Fig. 4, the contour of the stress is shown in two modes of loading: parallel and perpendicular to the major dimension of the cells. As it can be seen, in the first mode the stress concentration around the cell is less than that in the second one. The stress field shown in Fig. 4, when influenced by the stress field around the other cells (Fig. 3), intensifies the stress concentration phenomenon. These zones are sensitive to the more intensive localized deformation and crack growth, which is confirmed by experimental results [16].

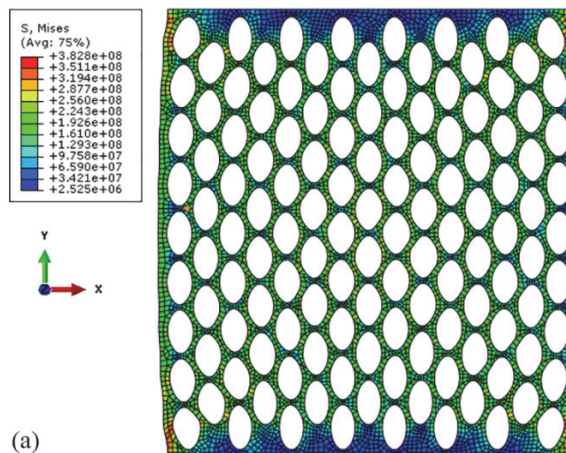


Fig. 3. The contour of the stress for  $R = 1.91$  after 0.5 mm displacement in two loading directions a) Y and b) X.

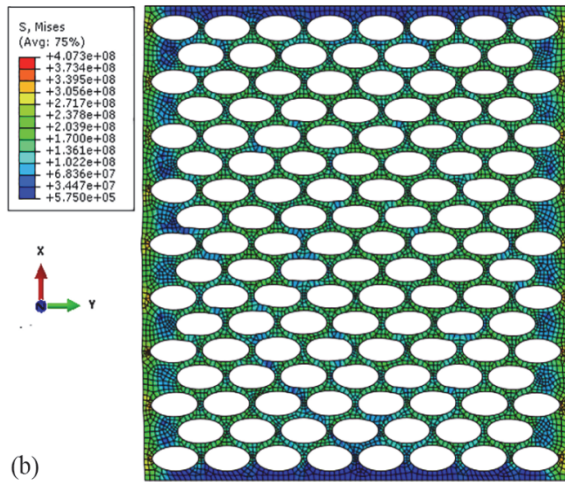


Fig.3. Continue

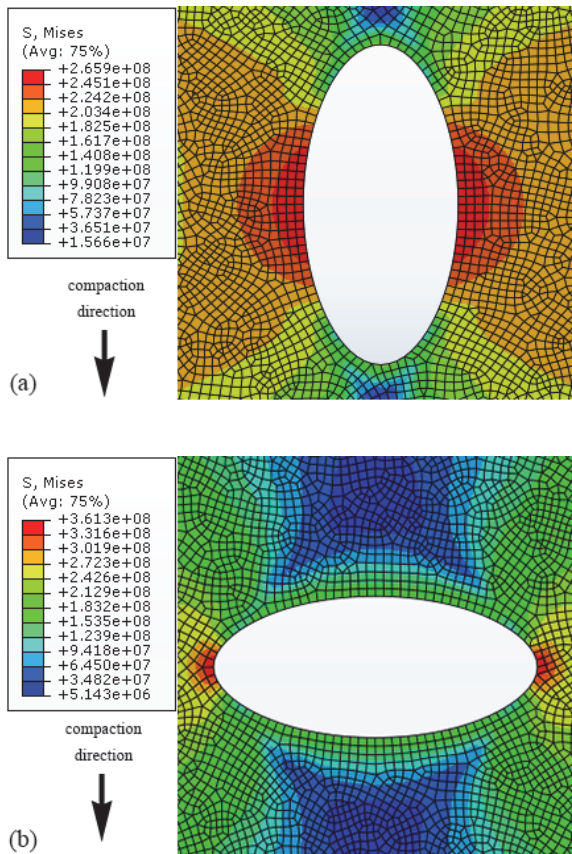


Fig. 4. Stress contour for twoQQ3 different loading directions a) Parallel and b) Perpendicular to the major dimension of the cell.

Figure 5 shows the variation in the yield strength ratio ( $\sigma_x/\sigma_y$ ) with R. As it can be seen, changes are similar to what predicted by Eq. 3. So by increasing R, the yield strength ratio also increases. However, there is some deviation from Eq. 3, which is due to the two-dimensionality of the model used in this study. In addition, the 2D FE analysis is under the plane strain condition and studies have shown that 2D models predict higher von Mises stress and equivalent plastic strain exceeding a certain value [17]. Fig. 6 shows the variation in the elastic tangent ( $E_x/E_y$ ) with R. Unlike the yield strength ratio, here, for the elastic tangent ratio, the results of the 2D modeling have a relatively good fit with the prediction of Eq. 2.

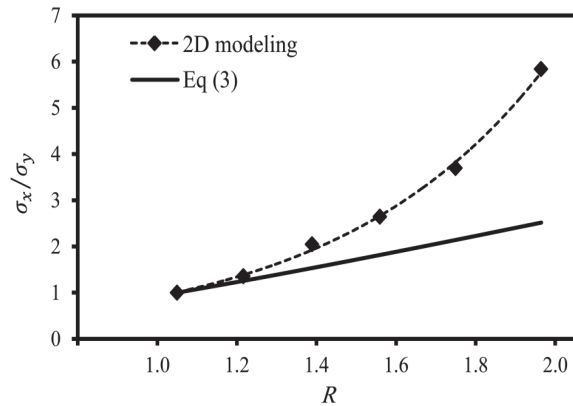


Fig. 5.  $\sigma_x/\sigma_y$  as a function of R in two modes of modeling and comparison with the prediction of Eq. 3.

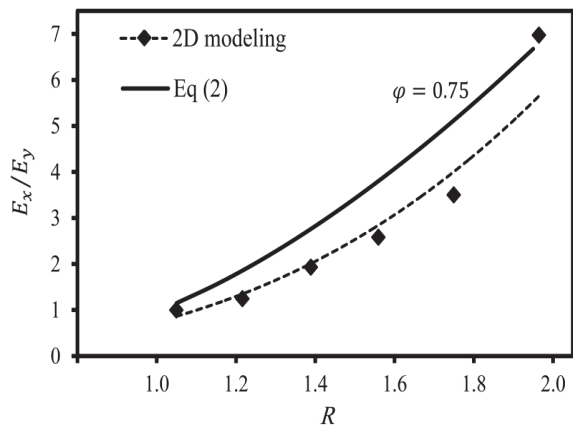


Fig. 6.  $E_x/E_y$  as a function of R in two modes of modeling and comparison with the prediction of Eq. 2.

In the powder-space holder process, the foam made using spherical spacer particles tends to an elliptical shape in the powder compression step. This phenomenon has been reported by different researchers [18,19]. In some cases, the deformation is as high as  $R$  equal to 1.3 [9]. Fig. 7 shows the longitudinal cross-section (parallel to the compaction direction) for regular cell arrangement of porous 316L stainless steel, which indicates the deformation of the cells. In this case, it is suggested that the compressive loading is applied in a direction vertical to the compaction direction, in order to obtain more favorable mechanical properties.

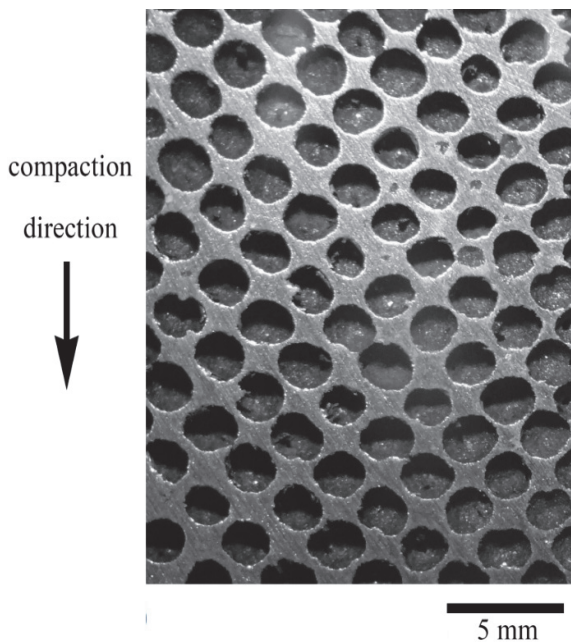


Fig. 7. The longitudinal cross-section of regular cell distribution of porous 316L stainless steel [9]. (reprinted with permission from Elsevier.)

Figure 8 shows the variation of the yield strength and the elastic tangent with  $R$  when the angle between the compression loading and the Y-axis is  $45^\circ$ . As it is shown, these two parameters are maximum when  $R$  is equal to 1, that is, the shape of the cells is spherical. In contrast, they are minimum by increasing  $R$ , as the shape of the cells is far from spherical. These results are due to the anisotropy created from the regular distribution of the cells.

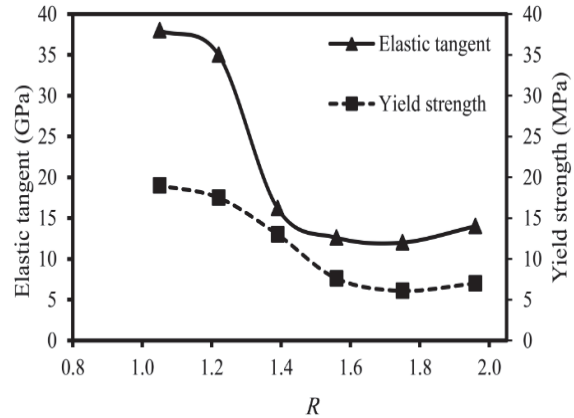


Fig. 8. Variation of elastic tangent and yield strength with  $R$  in the loading mode of  $45^\circ$  to the Y-axis direction.

Figure 9 shows the contour of the stress for different  $R$  values after 0.5 mm displacement. When  $R$  reaches 1, the contour of the stress is more uniform and symmetrical. As the amount of  $R$  increases, the stress contour becomes asymmetric to the extent that the stress is higher in the direction of the major dimension of the cells.

In fact, the mechanical properties of the foam decrease markedly by increasing the major dimension of the cell in a direction that has  $45^\circ$  angle difference with the loading direction. The maximum shear stress in a uniaxial compression test occurs on a plane at  $45^\circ$  to the loading direction because the maximum shear stress plane overlaps with the more stress concentration plane due to the shape of the cells during compression loading.

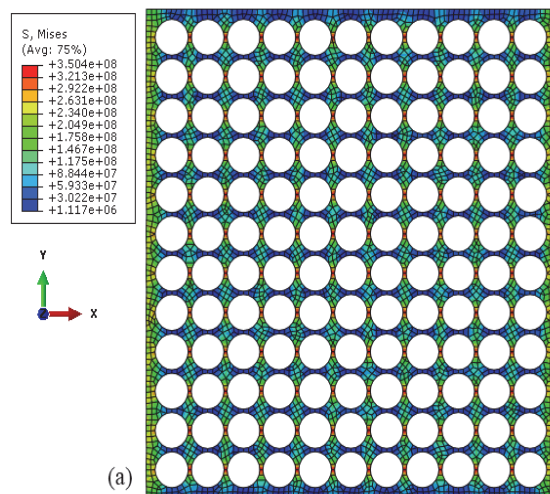


Fig. 9. Stress contour after 0.5 mm displacement in y-axis for different  $R$  values: a) 1, b) 1.34, c) 1.7 and d) 1.9.

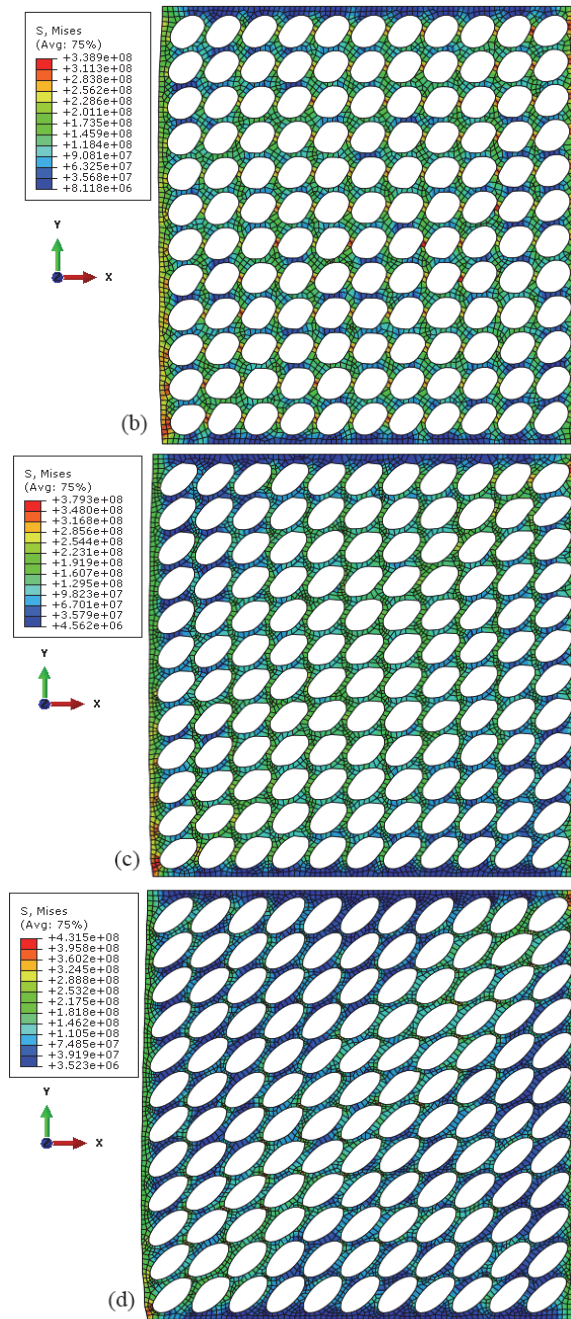


Fig.9. Continue

## 5. Conclusions

The simultaneous influence of the shape and regular cell distribution on the elastic properties of 316L stainless steel foam was investigated. The results showed that the anisotropy is present in properties such as elastic tangent and yield strength in both cases. When the shape of the cells changes from spherical to elliptic, the

mechanical properties are more favorable in the major dimension of the cell. In contrast, the foam with spherical cells has the same properties in two directions: x and y, but when the load is in a 45° of the Y-axis direction (e.g. the foam with elliptical cells), the mechanical properties will change.

Regarding these results, it can be concluded that the effect of the shape and distribution of the cells on the improvement of the mechanical properties is affected by two phenomena: Firstly, the reduction of the stress concentration during loading due to the cell shape, and secondly the maximum shear stress plane that does not overlap with the highest cell concentration plane.

## 6. References

- [1] E.A. Basir, K. Narooei, Simulation of Deformation Behavior of Porous Titanium Using Modified Gurson Yield Function, *Iran. J. Mater. Form.*, 3 (2016) 26–38. doi:10.22099/IJMF.2016.3861.
- [2] N. Bekoz, E. Oktay, Mechanical properties of low alloy steel foams: Dependency on porosity and pore size, *Mater. Sci. Eng. A*, 576 (2013) 82–90. doi:10.1016/j.msea.2013.04.009.
- [3] a.-H.H. Benouali, L. Froyen, T. Dillard, S. Forest, F. N'guyen, F. N'Guyen, Investigation on the influence of cell shape anisotropy on the mechanical performance of closed cell aluminium foams using micro-computed tomography, *J. Mater. Sci.*, 40 (2005) 5801–5811. doi:10.1007/s10853-005-4994-9.
- [4] Y. Mu, G. Yao, H. Luo, Effect of cell shape anisotropy on the compressive behavior of closed-cell aluminum foams, *Mater. Des.*, 31 (2010) 1567–1569. doi:10.1016/j.matdes.2009.09.044.
- [5] Y. Mu, G. Yao, Anisotropic compressive behavior of closed-cell Al-Si alloy foams, *Mater. Sci. Eng. A*, 527 (2010) 1117–1119. doi:10.1016/j.msea.2009.09.045.
- [6] Y. Mu, G. Yao, H. Luo, Anisotropic damping behavior of closed-cell aluminum foam, *Mater. Des.*, 31 (2010) 610–612. doi:10.1016/j.matdes.2009.06.038.
- [7] A. Manonukul, P. Srikudvien, M. Tange, C. Puncreobutr, Geometry anisotropy and mechanical property isotropy in titanium foam fabricated by replica impregnation method, *Mater. Sci. Eng.* 655 (2016) 388–395. doi:10.1016/j.msea.2016.01.017.

- [8] M. Mirzaei, M.H. Paydar, Compressive behavior of double-layered functionally graded 316L stainless steel foam, *Int. J. Mater. Res.*, 109 (2018) 938–943. doi:10.3139/146.111689.
- [9] M. Mirzaei, M.H. Paydar, A novel process for manufacturing porous 316 L stainless steel with uniform pore distribution, *Mater. Des.*, 121 (2017) 442–449. doi:10.1016/j.matdes.2017.02.069.
- [10] L.J. Gibson, M.F. Ashby, Cellular solids: structure and properties, Cambridge university press, 1999.
- [11] A. Elmoutaouakkil, L. Salvo, E. Maire, G. Peix, 2D and 3D Characterization of Metal Foams Using X-ray Tomography, *Adv. Eng. Mater.*, 4 (2002) 803–807. doi:10.1002/1527-2648(20021014)4:10<803::AID-ADEM803>3.0.CO;2-D.
- [12] K. McCullough, N. Fleck, M. Ashby, Uniaxial stress–strain behaviour of aluminium alloy foams, *Acta Mater.*, 47 (1999) 2323–2330. <http://www.sciencedirect.com/science/article/pii/S1359645499001287> (accessed September 7, 2016).
- [13] R.K. Desu, H.N. Krishnamurthy, A. Balu, A.K. Gupta, S.K. Singh, Mechanical properties of austenitic stainless steel 304L and 316L at elevated temperatures, *J. Mater. Res. Technol.*, 5 (2016) 13–20.
- [14] I. Standard, INTERNATIONAL STANDARD Mechanical testing of metals - Ductility testing-Compression test for porous and cellular metals, 2011 (2011).
- [15] R.W. Hertzberg, R.P. Vinci, J.L. Hertzberg, Deformation and Fracture Mechanics of Engineering Materials, 5th Edition, Wiley, 2012. <https://books.google.com/books?id=8d8bAAAAQBAJ>.
- [16] M. Mirzaei, M.H. Paydar, Fabrication and Characterization of Core–Shell Density-Graded 316L Stainless Steel Porous Structure, *J. Mater. Eng. Perform.*, (2018). doi:10.1007/s11665-018-3797-5.
- [17] H. Shen, L.C. Brinson, Finite element modeling of porous titanium, *Int. J. Solids Struct.*, 44 (2007) 320–335. doi:10.1016/j.ijsolstr.2006.04.020.
- [18] M. Alizadeh, M. Mirzaei-Aliabadi, Compressive properties and energy absorption behavior of Al–Al<sub>2</sub>O<sub>3</sub> composite foam synthesized by space-holder technique, *Mater. Des.*, 35 (2012) 419–424. doi:10.1016/j.matdes.2011.09.059.
- [19] B. Jiang, N. Zhao, C. Shi, J. Li, Processing of open cell aluminum foams with tailored porous morphology, *Scr. Mater.*, 53 (2005) 781–785. doi:10.1016/j.scriptamat.2005.04.055.

## ناهمسانگردی در خواص الاستیک فوم فولاد زنگ نزن ۳۱۶L ناشی از شکل و توزیع منظم حفره‌ها

مرتضی میرزایی، محمدحسین پایدار

دانشکده مهندسی، بخش مهندسی مواد، دانشگاه شیراز، شیراز، ایران.

### چکیده

در این تحقیق با استفاده از روش مدل‌سازی دو بعدی اجزاء محدود، اثر شکل و توزیع منظم حفره‌ها بر خواص الاستیک فوم فولاد زنگ نزن ۳۱۶L بررسی شد. بدین منظور، منحنی تنش- کرنش فشاری با کمک یک مدل هندسی و داده‌های این آلیاژ در حالت بدون فوم پیش‌بینی شد. نتایج نشان داد که شیب ناحیه الاستیک و تنش تسلیم افزایش محسوس پیدا می‌کند وقتی که جهت بارگذاری فشاری موازی با جهت بعد بزرگ‌تر حفره است. همچنین، توزیع منظم حفره‌ها بر خواص فوق‌تأثیر داشته و کاهش شدیدی دارد وقتی که صفحه ماکزیمم تنش برشی منطبق بر صفحه با تراکم بیشتر حفره باشد. به علاوه، مدل‌سازی با روش اجزاء محدود نشان داد که خواص الاستیک فوم فولاد زنگ نزن ۳۱۶L به صورت ناهمسانگرد است و حالت بهینه شدیداً وابسته به شکل حفره و جهت بارگذاری در حالت توزیع منظم حفره‌ها است.

**واژه‌های کلیدی:** شکل حفره، توزیع منظم حفره، ناهمسانگردی، فوم فولاد زنگ نزن ۳۱۶L